meso-[2.2]Paracyclophanyltriphenylporphyrin: Electronic Consequences of Linking Paracyclophane to Porphyrin

L. Czuchajowski,*,† J. E. Bennett,‡ S. Goszczynski,†,§ D. E. Wheeler,† A. K. Wisor,†,⊥ and T. Malinski*,‡

Contribution from the Department of Chemistry, University of Idaho, Moscow, Idaho 83843, and the Department of Chemistry, Oakland University, Rochester, Michigan 48309-4401.
Received March 15, 1988

Abstract: (*R*+*S*)-*meso*-[2.2]Paracyclophanyltriphenylporphyrin, PCPP, a novel system in which the [2.2]paracyclophane unit, PCP, is directly connected with the porphyrin core, P, was characterized by spectroscopic, spectroelectrochemical, and electrochemical methods. The conformational analysis (MINDO/3 and CNDO/2) suggested the interplanar paracyclophane–porphyrin angle of 141.7°. The influence of the PCP unit on the electronic structure of the porphyrin compared to *meso*-tetraphenylporphyrin, TPP, is marked (CNDO/S) by an increase in energy of the HOMO and HOMO-1 of the porphyrin core and the filling of the energy gap in P levels by the highest occupied MOs of PCP. Singly excited configurations appear from the HOMO and HOMO-1 of PCP to the LUMO and LUMO+1 of P in the split excited B states of PCPP. Both calculated and experimental data point to bathochromic shifts in all Q and B excited states, with shifts increasing in the order P < TPP < PCPP. The role played by the P–PCP interaction increases in the B excited states. This interaction represents one-half of the CT% numbers in the excited B state for which the charge transfer from PCP to P amounts to 0.38 e. Two one-electron reductions and three one-electron transfer oxidations, with the latter having a total of 2 F of charge transferred, were observed by voltammetric and spectroelectrochemical measurements. The oxidation processes are strongly influenced by acid–base equilibria and correspond to the gradual detachment of two electrons from the PCPP molecule. It is assumed that after the oxidation steps PCPP → $PCPP^{\bullet+}$ → $PCPP^{2+}$, the flow of two electrons from PCP to P combined with the detachment of two protons, results in the formation of a quinoid system of bonds, possibly even across the PCP–P link, in which one benzene ring of PCP is involved. The results of the calculations for the accepted model favor this assumption. Oxidation of PCPP is followed by a polymerization process which leads to the formation of conductive film on the electrode. Thin-layer UV–visible spectra of oxidized PCPP show an appearance of a new charge-transfer band at 683 nm with molar absorptivity 20% higher than the original Soret band.

Considerable attention has recently been focused on so called cyclophane porphyrins[1-3] where the porphyrin ring represents one of the stacked structural units of a bi- or trilayered macrocycle. However, no compounds are known where the structural units of a cyclophane are joined to the porphyrin ring. We have recently synthesized a compound of this type, a novel *meso*-tetrakis-[2.2]paracyclophanylporphyrin, T(PCP)P.[4a,b] Replacing the phenyl groups in *meso*-tetraphenylporphyrin (TPP) by [2.2]-paracyclophane (PCP) units should alter significantly the electronic structure of the porphyrin ring due to the electron-donating properties of the paracyclophane.[4c,d] The unusual electronic structure of the latter, which includes transannular interactions, is responsible for additional effects after junction with the porphyrin, and current studies with this porphyrin have shown several interesting spectroscopic and electrochemical properties.[4b,5a,b] These include a significant negative shift (approximately 510 mV) of the oxidation potential in comparison to *meso*-tetraphenylporphyrin, a strong bathochromic shift of the Soret band, oxidative electropolymerization, and film formation. T(PCP)P thus provides the first example where a porphyrin free base can be oxidized in four steps to form a well-defined conductive polymeric film.[5b] The metalated analogues of this porphyrin therefore represent a new class of compounds where the redox properties of the metalloporphyrin system can be "tuned" over a much broader range of potentials than for tetraphenyl-substituted porphyrins. The polymeric films of tetra[2.2]paracyclophanylporphyrin show catalytic activity as well as photovoltaic effects[6] and therefore could be applicable in both electrocatalysis and in energy storage devices.

In order to fully elucidate the effects of the attachment of [2.2]paracyclophane to the porphyrin core, the need for a simpler analogue of T(PCP)P became apparent. With this realization, the synthesis of a novel compound, *meso*-mono[2.2]paracyclophanyltriphenylporphyrin, PCPP, was undertaken. This letter compound could be used to evaluate the influence of the pcp substituent in comparison to the phenyl substituent. In this paper, we report the electronic structure of this new cyclophanylporphyrin in view of quantum chemical calculations and the results of spectroscopic, electrochemical, and spectroelectrochemical studies. (*R*+*S*)-PCPP did not form crystals suitable for X-ray diffraction studies; therefore, it was necessary to base our theoretical calculations on the results of a geometry optimization procedure which is fully described below.

A further interest in the study of PCPP was to determine the correlation between the data obtained from quantum chemical calculations of the intermediates assumed for the redox processes and the data obtained from electrochemical and spectroelectrochemical experiments. In particular, these studies were focused on the heterogeneous electron-transfer phenomena from the PCPP to and from the electrode influenced by intramolecular electron transfer from the paracyclophanyl unit to the porphyrin core. This electron transfer, accompanied by chemical changes in the paracyclophanyl substituent, could then lead to the formation of a quinoid system of bonds. Some models were assumed which help to explain the changes taking place in the paracyclophanyl–porphyrin under both static and dynamic conditions.

† University of Idaho.
‡ Oakland University.
§ On sabbatical leave from Poznan Technical University, Poland.
⊥ Present address: Department of Chemistry, University of North Dakota, Grand Forks, ND 58202.

(1) Ward, B.; Wang, C.; Chang, C. K. *J. Am. Chem. Soc.* **1981**, *103*, 5236.
(2) Traylor, T. G.; Koga, N.; Deardurss, L. A.; Swepston, P. N.; Ibers, J. A. *J. Am. Chem. Soc.* **1984**, *106*, 5132.
(3) Hamilton, A.; Lehn, J. M.; Sessler, J. L. *J. Am. Chem. Soc.* **1986**, *108*, 5158.
(4) (a) Czuchajowski, L.; Lozynski, M. *J. Heterocycl. Chem.* **1988**, *25*, 349. (b) Czuchajowski, L.; Goszczynski, S.; Wisor, A. K. *J. Heterocycl. Chem.* **1988**, *25*, 1343. (c) Wisor, A. K.; Czuchajowski, L. *J. Phys. Chem.* **1986**, *90*, 1541. (d) Wisor, A. K.; Czuchajowski, L. *Monatsh. Chem.* **1983**, *114*, 1023.
(5) (a) Malinski, T.; Bennett, J. E.; Ciszewski, A.; Czuchajowski, L.; Edwards, W. D.; Wheeler, D. E. 196th ACS National Meeting, Los Angeles, CA, Sept. 25–30, 1988, INOR 302. (b) Malinski, T.; Bennett, J. E. Electrochemical Society Meeting, Honolulu, HI, 1987, Vol. 87-2, extended abstract 1285. (c) Ciszewski, A.; Hill, N.; Goszczynski, S.; Czuchajowski, L. 196th National ACS Meeting, Los Angeles, CA, Sept. 25–30, 1988, INOR 202.
(6) Czuchajowski, L.; Goszczynski, S.; Malinski, T.; Wheeler, D. E.; Wisor, A. K. *J. Heterocycl. Chem.*, in press.

0002-7863/89/1511-0607$01.50/0

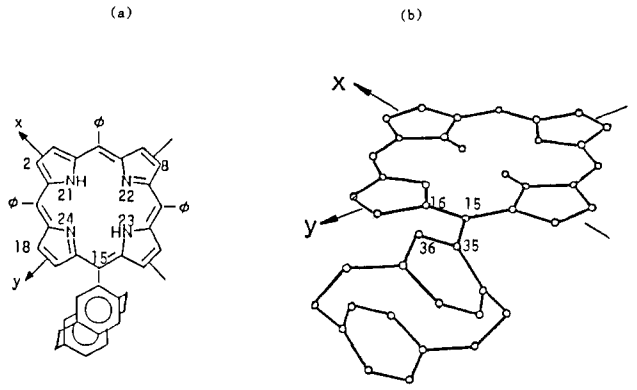

Figure 1. (a) *meso*-[2.2]Paracyclophanyltriphenylporphyrin, PCPP, under consideration. (b) Definition of the rotation (dihedral) angle: θ = C16–C15–C35–C36.

Theoretical Approach

Due to the substantial size of PCPP and other porphyrin systems considered (e.g., PCPP contains 98 atomic centers and 272 AOs), semiempirical quantum chemistry methods in an all-valence-electron approximation had to be applied in these studies. In all calculations the identical porphyrin skeleton of D_{2h} symmetry was assumed. Its geometry based on X-ray diffraction data[7] was taken from Schaffer and Gouterman[8] (oppositely located H atoms of the NH groups were situated on the *x*-axis). In *meso*-tetraphenylporphyrin, TPP, phenyl substituents are perpendicular to the *x*–*y* plane of the porphyrin core. In PCPP, the location of the three phenyl rings was assumed the same as in TPP. The geometry of the [2.2]paracyclophanyl substituent, PCP, was assumed according to the crystallographical data of the [2.2]-paracyclophane molecule.[9] The conformational states of PCPP which could originate from the various possible orientations of the inter-deck plane of PCP against the plane of the porphyrin core, Figure 1, were found by a geometry optimization procedure by using the force field method.[10] Conformational analysis was carried out via the CNDO/2[11] and MINDO/3[12] methods.

The electronic absorption spectra of PCPP and TPP were calculated by CNDO/S-CIS.[13] This latter method was successfully applied to the porphyrin by Maggiora and Weimann[14] and to the [2.2]paracyclophane by Wisor and Czuchajowski.[4c] The good results achieved for the porphyrin and the cyclophane with the CNDO/S method determined its application in the present research of PCPP. The calculations of the electronic spectra of PCPP were based on the results of conformational analysis. In the configuration interaction method (CI), 150 singly excited configurations of the lowest energy were considered for TPP and 200 configurations for PCPP. For this number of configurations their energetic criterion is similar and amounts to 75 000 cm^{-1}. In the framework of this criterion, one mixes the most important configurations of both the porphyrin and the [2.2]paracyclophane.

The characteristics of the excited states based on the transition density matrix method[15,16] was performed in the way described in recent papers by the authors.[4b,17] The oscillator strengths were calculated by using the dipole length operator including the charge terms and the one-center polarization terms.[11,13] The neglect of the two-center bond terms have been shown to have only a minor effect on the calculated oscillator strength values within this scheme. The authors' versions of programs in FORTRAN were applied. To matrix diagonalization the procedure of Householder-QR-Inverse-Interaction[18a] modified by one of the authors (A.K.W.)[18b] was applied. All calculations were performed on both the IBM and CRAY systems, the latter in the framework of a supercomputer network.

Experimental Section

Chemicals and Materials. *meso*-[2.2]-Paracyclophanetriphenylporphyrin, PCPP, was obtained following the Adler et al. method,[19a] by mixed condensation in propionic acid (350 mL, reflux for 1 h) of pyrrole (2.8 mL, 40 mmol in 50 mL of propionic acid) with benzaldehyde (3.2 mL, 30 mmol) and [2.2]paracyclophane-4-carbaldehyde[19b] (2.36 g, 10 mmol). The separational procedure described in detail elsewhere[6] consisted of two column chromatography steps (silica gel, solution in 1,2-dichloroethane/chloroform, 1:1, dichloromethane/ethyl acetate, 9:1, as eluent; Florisil, solution in 1,2-dichloroethane, dichloromethane as eluent) and a final TLC step (Kiesel gel Merck plates, 1-bromobutane as developer, isolation of PCPP as the R_f 0.55–0.60 band): 1.6% yield from the starting pyrrole; $C_{54}H_{40}N_4$ 744.9 calcd mass (M), 746 (M + H^+); ^1H NMR ($CDCl_3$) −2.64 (s, 2 H, NH), 2.21–3.62 (set of m, 8 H, CH_2 in PCP), 6.76–6.89 (m, 5 H, PCP), 7.01 (d, 1 H, PCP), 7.23 (d, 1 H, PCP), 7.77 and 7.90 (m and s, respectively, 9 H meta + para, Ph), 8.13, 8.20, 8.31, 8.39 (all m, 6 H ortho, PCP), 8.62 (s, 2 H, β-pyrrole), 8.82 (m, 4 H, β-pyrrole), 9.15 (d, 1 H, β-pyrrole), 10.14 (d, 1 H, β-pyrrole);[6] UV–vis (benzene) λ_{max} nm 652, 596, 555, 519, and 424 (Soret band).

1,2-Dichloroethane, $EtCl_2$, for electrochemical use, was purchased from Fisher Scientific Company as HPLC grade and was twice distilled from P_2O_5 before use. Spectroscopic grade *N*,*N*-dimethylformide (Aldrich) was vacuum distilled from activated 0.4 nm molecular sieves. The supporting electrolyte tetrabutylammonium perchlorate, TBAP, obtained from Eastman was twice recrystallized from ethanol, dried, and stored in vacuo at 45 °C. Aqueous 25% tetraethylammonium hydroxide (TEAH) solution was obtained from Eastman and used as received.

Electrochemical Methods. Cyclic voltammetric and differential pulse voltammetric measurements were made with an IBM EC225 voltammetric analyzer. An omnigraphic Houston 1000 X-Y recorder was used to record the current voltage output for sweep rates between 0.002 and 0.30 V/s. Current voltage curves taken at sweep rates between 0.40 and 10.0 V/s were collected on a digital storage oscilloscope with an X-Y recorder attached. Coulometric measurements were performed with a PAR Model 173 potentiostat/galvanostat and Model 179 digital coulometer. A conventional three-electron system was used. This consisted of a platinum working electrode (diameter 1 mm), a platinum wire counter electrode, and saturated calomel electrode (SCE) as the reference electrode. Aqueous SCE was separated from nonaqueous solvent by a fritted bridge containing supporting electrolyte and solvent.

UV–visible spectra were obtained with a Tracor Northern multichannel analyzer. The system was composed of a Tracor Northern 6050 spectrometer containing a crossed Czerny–Turner spectrograph and a Tracor Northern 1710 multichannel analyzer. Spectra were recorded from 279 to 891 nm by a double-array detector. Spectroelectrochemistry was performed in a bulk cell as well as in a thin-layer cell. The bulk cell followed the design of Fajer et al.[20] and had an optical path length of 0.19 cm. The thin-layer cell was built following the design of Lin et al.[21] with a calculated path length of 0.5 mm and platinum mesh as a working electrode. Values of λ are accurate to ±0.2 nm, while ε is good to ±2% of the absolute value presented.

(7) (a) Hoard, J. L.; Hamor, M. J.; Hamor, T. A. *J. Am. Chem. Soc.* **1963**, *85*, 2334. (b) Webb, L. E.; Fleisher, E. B. *J. Am. Chem. Soc.* **1965**, *87*, 667. (c) Silvers, S.; Tulinsky, A. *J. Am. Chem. Soc.* **1964**, *86*, 667.
(8) Schaffer, A. M.; Gouterman, M. *Theor. Chim. Acta* **1972**, *25*, 62.
(9) (a) Brown, C. J. *J. Chem. Soc.* **1953**, 3265. (b) Lonsdale, K.; Milledge, J.; Rao, K. V. K. *Proc. R. Soc. London Ser. A* **1960**, *225*, 82. (c) Hope, H.; Bernstein, J.; Trueblood, K. N. *Acta Crystallogr., Sect. B* **1972**, *28*, 1733.
(10) (a) Nalewajski, R.; Goleblewski, A. *Acta Phys. Pol. Ser. A* **1976**, *49*, 683. (b) Nalewajski, R. *J. Mol. Struct.* **1977**, *40*, 247.
(11) (a) Pople, J. A.; Santry, D. P.; Segal, G. A. *J. Chem. Phys.* **1965**, *43*, S129. (b) Pople, J. A.; Segal, G. A. *J. Chem. Phys.* **1965**, *43*, S136. (c) Pople, J. A.; Segal, G. A. *J. Chem. Phys.* **1967**, *47*, 158.
(12) (a) Bingham, R. C.; Dewar, M. J. S.; Lo, D. H. *J. Am. Chem. Soc.* **1975**, *97*, 1285, 1294, 1302, 1307. (b) Dewar, M. J. S.; Lo, D. H.; Ramsden, C. A. *J. Am. Chem. Soc.* **1975**, *97*, 1311.
(13) (a) Del Bene, J.; Jaffe, H. H. *J. Chem. Phys.* **1968**, *48*, 1807; **1968**, *48*, 4050; **1968**, *49*, 1221; **1969**, *50*, 563; **1969**, *50*, 1126. (b) Ellis, R. L.; Kuehnlenz, G.; Jaffe, H. H. *Theor. Chim. Acta* **1972**, *26*, 131. (c) Kuehnlenz, G.; Jaffe, H. H. *J. Chem. Phys.* **1973**, *58*, 2238.
(14) (a) Maggiora, G. M.; Weimann, L. J. *Chem. Phys. Lett.* **1973**, *22*, 297. (b) Maggiora, G. M.; Weimann, L. J. *Int. J. Quantum Chem.: QBS* **1974**, *1*, 179. (c) Maggiora, G. M. *J. Am. Chem. Soc.* **1973**, *95*, 6555.
(15) McWeeny, R.; Sutcliffe, B. T. *Methods of Molecular Quantum Mechanics*; Academic Press: London, New York, 1969.
(16) Luzanov, A. V. *Russ. Chem. Rev.* **1980**, *49*, 1033.
(17) Wisor, A. K.; Czuchajowski, L. *Theor. Chim. Acta*, in press.
(18) (a) Beppil, Y.; Nonomiya, I. *Comput. Chem.* **1982**, *6*, 87. (b) Wisor, A. K. *Comput. Chem.* **1986**, *10*, 307.
(19) (a) Adler, A. D.; Longo, F. R.; Finarelli, J. D.; Goldmacher, J.; Assour, J.; Korsakoff, L. *J. Org. Chem.* **1967**, *32*, 476. (b) Hopf, H.; Raulfus, F. W. *Isr. J. Chem.* **1985**, *25*, 210.
(20) Fajer, J.; Borg, D. C.; Forman, A.; Dolphin, D.; Felton, R. M. *J. Am. Chem. Soc.* **1970**, *92*, 3451.
(21) Lin, X. Q.; Kadish, K. M. *Anal. Chem.* **1985**, *57*, 1498.

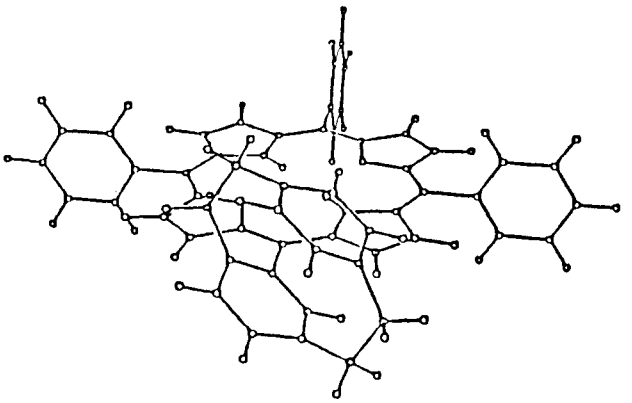

Figure 2. ORTEP drawing of the stable conformer of *meso*-[2.2]paracyclophanyltriphenylporphyrin.

Results and Discussion

Conformational Analysis. The lack of experimental data concerning the three-dimensional structure of PCPP gave particular importance to the applications of conformational analysis. It is well known, in such an approach, that some molecular fragments can be transferred from one molecule to another. In the case of PCPP these fragments represent the porphyrin core, [2.2]paracyclophane, and benzene rings. In the search for a stable conformation we assume a particular orientation of the phenyl rings against the porphyrin core plane and the possibility of PCP rotation along the PCP–porphyrin core bond. The rotation angle, θ, is the dihedral angle C(16)–C(15)–C(35)–C(36), see Figure 1. $\theta = 0°$ when the benzene ring of PCP (in fact—four C atoms in it) directly joined to the porphyrin is coplanar with the latter, while the second benzene ring connected with the first by ethane bridges is situated below it. θ increases for the clockwise rotation when the C(15)–C(35) bond is viewed from the porphyrin core to PCP.

Both applied methods, MINDO/3 and CNDO/2, point to the existence of one stable conformer of PCPP, characterized by $\theta = 141.7°$ (Figure 2) with an energy of −188 833.8 kcal/mol (MINDO/3), −289 299.10 kcal/mol (CNDO/2). The dependence of the energy of the conformer on the angle θ, calculated by both methods, shows that the change of θ by only 10° greatly increases its energy, 310 kcal/mol according to CNDO/2 and 170 kcal/mol according to MINDO/3. Finally, calculations showed only a small influence of the tautomeric equilibrium of the porphyrin core on the energy of the conformer. According to MINDO/3, when the hydrogen atoms of the central NH groups are localized on the "*y*" axis, the energy of the conformer decreases by 0.4 kcal/mol. The ^{1}H NMR (300 MHz) spectrum of PCPP in $CDCl_3$ shows, accordingly, only one signal of two NH protons at room temperature ($\delta = -2.64$).[6]

MO Structure. The influence of the phenyl and PCP substituents on the energy levels of the MOs for the porphine molecule, P, is presented in Figure 3. The MO diagram of P points to two facts already known:[14b] (i) The frontier MOs are the π-type orbitals (six highest occupied and all virtual orbitals shown in Figure 3), while the σ-type MOs are those of a_g and b_{2u} symmetry localized on the lone electron pairs of N atoms of the pyrrole rings situated below the occupied π-orbitals; (ii) the two highest occupied MOs of a_u (HOMO) and b_{1u} (HOMO−1) symmetry, like the two lowest virtual MOs b_{2g} (LUMO) and b_{3g} (LUMO+1), are separated from the remaining ones by a substantial energy gap. This separation is in agreement with the four-orbital model of Gouterman et al.,[22] in which the singly excited configurations interacting between these two pairs of MOs contribute more to the well-known excited states Q and B (corresponding to the longest wavelength and the Soret bands, respectively). In the case of TPP the set of orbital levels originating from P does not change substantially with the exception of the HOMO and HOMO−1 pair which show

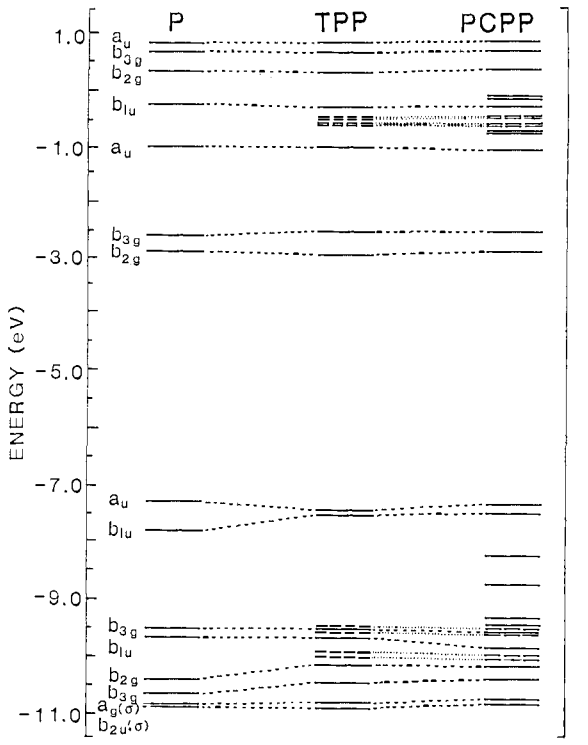

Figure 3. MO diagrams for porphine (P), *meso*-tetraphenylporphyrin (TPP), and *meso*-[2.2]paracyclophanyltriphenylporphyrin (PCPP).

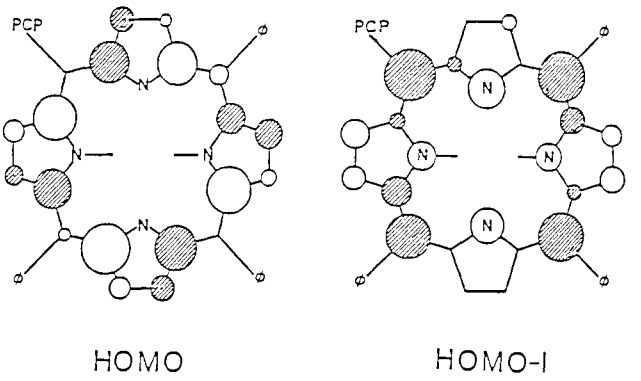

Figure 4. The atomic orbital (AO) structure of the porphyrin core of PCPP in the two highest occupied MOs. The size of the circles is approximately proportional to the AO coefficients. The view is looking down the positive *z* axis of the upper lobe of the p_z AO's. The white area indicates a positive value for the upper lobe, while the dark area indicates a negative value.

less splitting. New orbital levels appear which originate from the phenyl rings, and their location is almost the same as in benzene.[23] However, when compared to the latter, the degenerate pair of benzene HOMO's splits into two groups of orbitals, each containing four closely situated levels. A similar phenomenon occurs with the degenerate pair of benzene LUMO's. This is a result of limited interactions existing between the P and the phenyls. It is however, important to note that in the case of TPP, facts (i) and (ii) known for P are still valid.

The PCP substituent changes the MO diagram of PCPP: the HOMO and HOMO−1 increase in energy as compared to TPP. According to Koopman's theorem[24] ($IP_1 = -E_{HOMO}$), PCPP should have the first ionization potential lower than TPP. This tendency is readily observed in electrochemical oxidation, where the first half-wave potential of TPP is 1.05 V while that of PCPP is 0.95 V in $EtCl_2$. It is also worth noting that the greatest change of shape involves the HOMO, which results from the effect of the

(22) Gouterman, M. "Optical Spectra and Electronic Structure of Porphyrins and Related Rings" In *The Porphyrins*; Dolphin, D.; Ed.; Academic Press: New York, 1978; Vol. III, pp 1–165.

(23) Wisor, A. K.; Czuchajowski, L., unpublished results.
(24) Koopmans, T. *Physica* **1933**, *1*, 104.

Table I. Calculated and Observed Electronic Transitions of *meso*-[2.2]Paracyclophanyltriphenylporphyrin Compared to Porphine and *meso*-Tetraphenylporphyrin

	porphine (D_{2h})				*meso*-tetraphenylporphyrin				*meso*-[2.2]-paracyclophanyltriphenylporphyrin			
	calculated		observed		calculated		observed[d]		calculated		observed[e]	
state[a]	λ, nm	*f*	λ, nm	*f*	λ, nm	*f*	λ, nm	*f*[f]	λ, nm	*f*	λ, nm	*f*[f]
Q_x	701.4	0.009	617[b]	0.005[f]	708.3	0.017	647	0.019	721.5	0.008	652	0.025
			628[c]	0.006[c]								
Q_y	595.9	0.174	521[b]	0.017[f]	601.8	0.071	548	0.046	608.3	0.076	555	0.58
			512[c]	0.006[c]								
B_x	371.2	1.413			371.5	2.055			394.0	0.877		
			395[b]	1.479[f]					364.3	1.268		
			385[c]	1.4[c]			419	2.630			424	2.339
B_y	340.5	2.572			361.0	3.147			385.9	1.351		
									375.2	1.417		

[a] See ref 22 for a discussion of the nomenclature. [b] In benzene, ref 28. [c] In vapor, ref 29. [d] In benzene, ref 30. [e] In benzene, ref 6. [f] Calculated from $\log \epsilon = 5.25 + \log f$.

Table II. Analysis of Some Excited States of Porphine, *meso*-Tetraphenylporphyrin, and *meso*-[2.2]Paracyclophanyltriphenylporphyrin by Transition Density Matrix Method[a]

	porphine				*meso*-tetraphenylporphyrin						*meso*-[2.2]paracyclophanyltriphenylporphyrin							
state	l_B	LE%	$l_{B\text{-}Py}$	CT%	l_B	l_{Ph}	LE%	$l_{B\text{-}Py}$	$l_{Ph\text{-}Py}$	CT%	l_B	l_{Ph}	l_{PCP}	LE%	$l_{B\text{-}Py}$	$l_{Ph\text{-}Py}$	$l_{PCP\text{-}Py}$	CT%
Q_x	3.0	19.8	42.8	80.2	3.7	0.0	17.1	43.0	4.0	82.9	3.2	0.0	0.1	16.8	40.8	2.3	4.7	83.2
Q_y	5.0	25.2	24.4	74.8	6.5	0.0	23.9	26.6	4.0	76.1	5.9	0.0	0.1	22.7	24.6	2.2	4.4	77.3
B_x	1.6	27.4	30.0	72.6	1.6	0.8	21.0	31.0	3.2	79.0	0.8	0.3	3.3	17.4	15.5	0.2	41.6[b]	82.5
											1.5	0.5	0.5	21.4	22.3	1.3	12.9[b]	78.6
B_y	11.8	24.2	39.6	75.8	10.9	2.0	25.1	34.2	5.6	74.9	3.8	0.4	5.0	20.5	15.4	1.0	39.6[b]	79.5
											3.9	0.4	2.1	16.3	16.3	1.1	43.5[b]	83.7

[a] References 17 and 27. l_B, l_{Ph}, and l_{PCP} are the partial localization numbers giving the excitation (LE) on the bridges, phenyl, and PCP fragments, respectively. $l_{B\text{-}Py}$, $l_{Ph\text{-}Py}$, and $l_{PCP\text{-}Py}$ are the charge transfer (CT) localization numbers referring to the transfer from bridges, phenyl, and PCP to pyrrole fragments including reverse transfer, respectively. LE% is the sum of all partial localization numbers. CT% is the sum of all CT localization numbers; LE% + CT% = 100%. [b] Denotes mainly the transfer from PCP to P, the reverse transfer being negligible.

appearance of the electron population on the meso atom centers C(10) and C(20) (PCP is attached to C(15)), Figure 4.

The most essential fact, however, is the appearance of new orbital levels which in the case of occupied MOs fill the energy gap. These levels originate from PCP, and their location on the energy scale is not much different than in [2.2]paracyclophane alone.[23] One would expect that such contiguity of the highest occupied MOs of PCP and the HOMO and HOMO−1 of P, seen in Figure 3, would result in the appearance of configurations singly excited from the highest occupied orbitals of PCP to the LUMO and LUMO+1 of P in the Q and B excited states of PCPP (this problem is discussed more closely in another paragraph). Finally, the orbitals originating from the three phenyl rings do not change their location nor do those of σ-type orbitals when PCPP is compared to TPP. The above considerations are based on CNDO/S calculations. Similar results were obtained by both CNDO/2 and MINDO/3 methods.

The Singlet–Singlet Spectra. The investigation of electronic absorption spectra of porphyrins provides valuable information about the electronic structure of these systems.[22] Therefore, it is interesting to determine the degree to which the electronic structure of the porphyrin is modified as a result of the attachment of the [2.2]paracyclophanyl fragment. The [2.2]paracyclophane itself shows unusual physico-chemical properties originating mainly from transannular interactions,[25] as demonstrated also by two of the authors.[26,27] The results of the CNDO/S-CIS calculations for P, TPP, and the stable conformer of PCPP are shown in Table I. The data concern only the excited Q and B states. Other particularities of the spectra are discussed in a separate paragraph. While the electronic spectrum of P has already been investigated,[14a,b] our calculations concerning P are given in order to extend the basis of comparison between the spectra of PCPP and TPP.

In the UV–vis spectra, the gradual bathochromic shift of all bands takes place in the following order: P < TPP < PCPP, and some of these changes are listed in Table I. The greatest changes result from the attachment of four phenyls to the porphyrin core, while smaller changes follow the exchange of one of these phenyls by PCP. The general trend seen in the band shifts, porphine → TPP → PCPP, is also observed in the calculations presented and qualitatively correlates very well. The calculated transitions to Q and B excited states occur at increasing wavelength values in the same order, P < TPP < PCPP. However, the quantitative aspect of the bathochromic shifts is not satisfactory, and no general agreement of the observed intensities of bands with the calculated oscillator strengths has been reached. The results are only correct for the short wavelength A → B transitions.

Quantum chemistry calculations create the possibility of interpretations at the various types of electronic transitions, and, as a result of this, some important conclusions have been reached. In PCPP, the split of excited states appears to correspond to the short wavelength A → B transition. The lack of this effect in TPP proves that it is related to the replacement of the phenyl ring by PCP. The analysis of the CI coefficients for the B excited states supports our previous assumption (see above) that some excited states of PCPP participate in configurations singly excited from the occupied MOs localized on PCP to the LUMO and LUMO+1 of P. In the two excited states considered, these configurations participate more or less to the same extent as configurations singly excited from the HOMO and HOMO−1 of P to its LUMO and LUMO+1. The calculated split of the short wavelength A → B transition is found in the broadening (by ca. 15%) of the Soret band in PCPP as compared to TPP. The calculated oscillator strengths for these transitions are similar but smaller by one-half then corresponding transitions in TPP. Although the observed intensity of the Soret band in PCPP is accordingly smaller than in TPP, this decrease is less pronounced than the calculations would suggest. Similar characteristics are valid for P,[14] where two components of the short wavelength transition A → B_x and A → B_y are split only by 564 cm^{-1}.[31] Presumably, the analogous

(25) (a) Cram, D. J. *Rec. Chem. Progr.* **1959**, *20*, 71. (b) Cram, D. J.; Cram, J. M. *Acc. Chem. Res.* **1971**, *4*, 204.
(26) Czuchajowski, L.; Wisor, A. K. *J. Electron Spectrosc. Relat. Phenom.* **1987**, *43*, 169–181, and ref 2–7, 9, 10 therein.
(27) Czuchajowski, L.; Wisor, A. K. *J. Mol. Struct. (Theochem)* **1988**, *165*, 163.

(28) Eisner, V.; Linstead, R. P. *J. Chem. Soc.* **1955**, 3749.

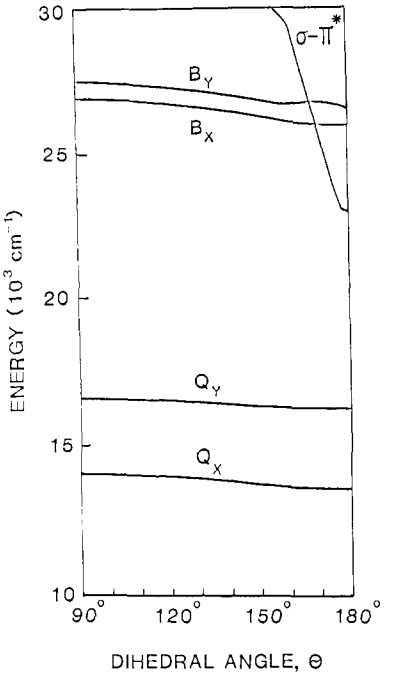

Figure 5. Energy of the lowest excited states of TPP vs rotation angle of one phenyl ring (three others remain perpendicular against porphyrin core).

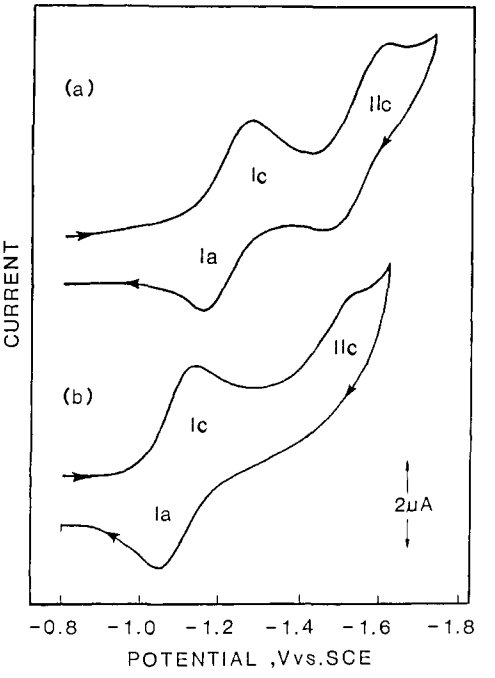

Figure 6. Cyclic voltammogram of PCPP: (a) in 1,2-dichloroethane containing 0.1 M TBAP and (b) in 1,2-dichloroethane containing 0.1 M TBAP and 1 μM of TEAH. Scan rate = 100 mV/s.

situation exists for the split excited A → B transition in PCPP.

The analysis of the excited states by the transition density matrix method[15,16] reflects, also, the influence of PCP, see Table II. The various porphyrin molecules are divided, in this treatment, into the following fragments: four pyrrole rings, four methine bridges, four phenyl rings for TPP, and three phenyls and one PCP unit for PCPP. The LE% numbers represent the weight of the states locally excited on all molecular fragments, and the CT% numbers represent the weight of charge-transfer states between these fragments. For the excited Q states, no substantial changes in the magnitude of LE% and CT% appear, except for the increase of CT% on the account of LE% in the following order: P < TPP < PCPP. This points to a limited influence of the phenyl or PCP substituents on the Q excited states. More pronounced changes characterize the B excited states. Responsible for the changes in CT% numbers is the increase of the interaction between P and the PCP substituent. The effect is strongest for PCPP, where the ratio of porphyrin–PCP interaction represents one-half of the CT% numbers in the doubly excited B state. Also, the size of the charge transferred from PCP to P, 0.38 e, is meaningful in this respect.

Modelling Spectral Changes in PCPP as Compared to TPP. In comparison of PCPP with TPP, the question arises to what extent do the spectral changes in PCPP originate from the rotation of the PCP substituent with regard to the plane of the porphyrin core. Also one should ask the question to what extent the spectral changes originate from the particular nature of PCP itself. We calculated, therefore with CNDO/S, the influence of the rotation of one phenyl ring, out of the four present in TPP, on the energy of the lowest Q and B excited states for the dihedral (rotation) angle θ changing from 90° to 0° or 90° to 180° depending on the direction of rotation, with the final structure representing the coplanar arrangement. The results presented in Figure 5 show that (i) along with the rotation, the energy of the Q and B states gradually decreases, (ii) the greatest changes of excitation energy appear for θ 120°–150° with B > Q, (iii) the split of the X and Y components of the B and Q states retains a constant level, and

(29) (a) Edwards, L.; Dolphin, D. H.; Gouterman, M. *J. Mol. Spectrosc.* **1970**, *35*, 90. (b) Edwards, L.; Dolphin, D. H.; Gouterman, M.; Adler, A. D. *Ibid.* **1971**, *38*, 16.

(30) Badger, G. M.; Jones, R. A.; Laslett, R. L. *Aust. J. Chem.* **1964**, *17*, 1028.

(31) Sevchenko, A. N.; Solvlev, K. N.; Mashenko, V. A.; Shkirman, S. F. *Sov. Phys. Dokl.* **1966**, *10*, 778.

Table III. Half-Wave Potentials (V vs SCE) for the Redox Reactions of PCPP in Different Solvents[e]

solvent	reduction waves I	reduction waves II	oxidation waves III	oxidation waves IV	oxidation waves V	oxidation waves VI
$EtCl_2$	−1.24	−1.53	0.95	1.18[a]	1.42	1.72[d]
$EtCl_2$ + 1 μM TEAH	−1.10	−1.51[b]		1.25[a,c]		1.59[d]
$EtCl_2$ + 1 μM AcA	−1.21	−1.53	0.97		1.40	
DMF	−1.05	−1.51	1.02[a]	1.12[a]		1.60[d]

[a] Anodic peak potential. [b] Cathodic peak potential. [c] Wave III and IV. [d] Based on DPV measurements. [e] Supporting electrolyte—TBAP; scan rate 0.1 V/s.

(iv) for θ 160°–180° an excited σ–π^* state appears which is characterized by low intensity and rapidly decreasing energy located in the vicinity of the B states. The first three results are valid for PCPP and are confirmed by (iv), which points to the importance of mutual rotation of the planes of PCP and P. The value of θ in PCPP, suggested by conformational analysis (141.7°) which served as the basis for the calculation of the electronic spectrum, is contained within the range of calculated θ values characteristic for TPP, i.e., 120°–150°, for which the energy changes in the excited states are the greatest. The similarity of θ values and of the direction of energy changes for the excited states shows that, above all, the rotation is responsible for the observed spectral changes and is independent of the type of substituent, phenyl or PCP. However, the situation in which the phenyl ring(s) is not perpendicular to the porphyrin plane does not exist in TPP, and therefore spectral changes become possible only when the phenyl ring is replaced by PCP. This leads us, in turn, to the conclusion that both the character and the rotation of the PCP substituent are responsible for the spectral changes observed in PCPP.

Reduction of PCPP—Voltammetry and Spectroelectrochemistry. Figure 6a illustrates a typical cyclic voltammogram of PCPP in $EtCl_2$ (0.1 M TBAP). As seen in this figure, two reduction processes occur at −1.24 and −1.53 V versus SCE (labeled I_c and II_c). Half-wave potentials of these redox couples are listed in Table III. The observed currents for the two reductions are equal in height with the peak separations in the cyclic voltammogram for the first peak $E_{pa} - E_{pc} = 60 \pm 5$ mV, while for the second peak $E_{pa} - E_{pc} = 70 \pm 5$ mV (scan rate $v = 0.1$ V/s). A constant value of $i_p/v^{1/2}$ was obtained indicating one electron is reversibly or

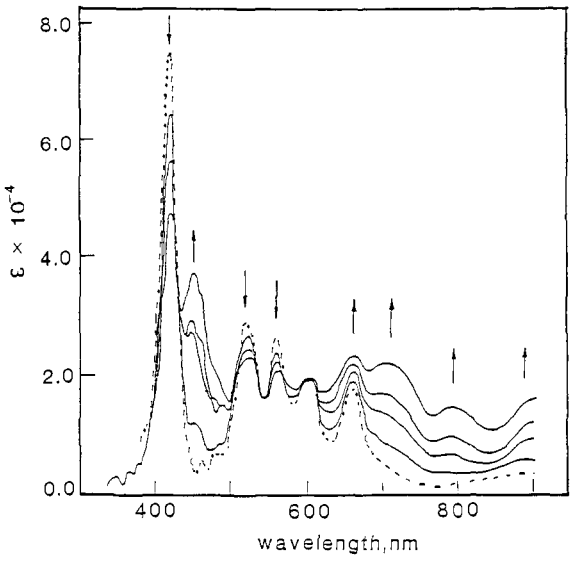

Figure 7. Thin-layer electron absorption spectra for reduced PCPP in 1,2-dichloroethane (0.1 M TBAP). The dashed line shows the spectrum before electrolysis.

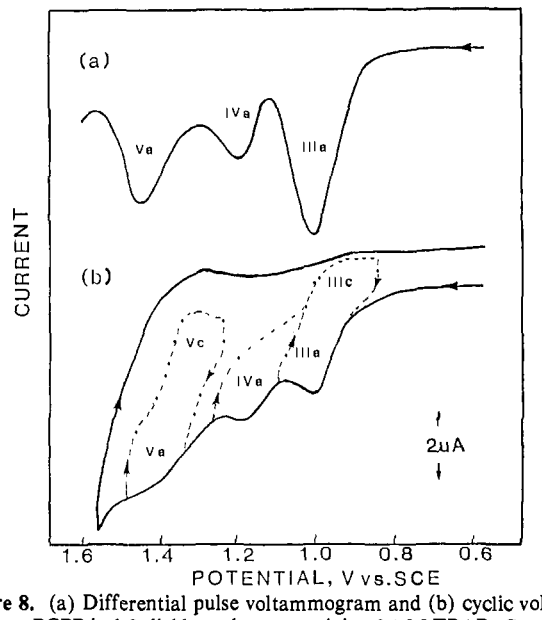

Figure 8. (a) Differential pulse voltammogram and (b) cyclic voltammogram PCPP in 1,2-dichloroethane containing 0.1 M TBAP. Scan rate = 5 and 100 mV/s, respectively.

quasi-reversibly transferred in each step and that both electrode processes are diffusion controlled.[32] The first reduction involves a one-electron addition which is reversible during an electrolysis time less than 30 s as evidenced by the fact that reoxidation could be accomplished at −0.7 V with the abstraction of one electron. The second one-electron reduction of PCPP is irreversible on the controlled potential electrolysis time scale. Spectral changes recorded during thin-layer spectroelectrochemistry are shown in Figure 7. The molar absorptivity of the Soret band is greatly affected and reduced in the presence of the supporting electrolyte, TBAP, while the molar absorptivities of the other bands are affected to a lesser extent. This is reflected by the molar absorptivities shown in Figure 7 when these values are compared with the log values presented in ref 6. An original spectrum of PCPP in $EtCl_2$, 0.1 M TBAP shows five bands. The Soret band is observed at 421 nm with the remaining four bands at 523, 558, 598, and 658 nm, respectively. These positions differ from those in the Experimental Section and in ref 6 due to the differences in the solvents used. During the first step of reduction (wave I), the Soret band at 421 nm decreases slightly, while several new bands appear at 453, 698, 726 (sh), and 786 nm, Figure 7. This spectrum can be attributed to the porphyrin anion radical $[PCPP^{\bullet}]^{-}$. The final spectrum obtained after the second reduction of PCPP has a significantly decreased Soret band as well as a decreased set of bands at 523 and 558 nm. A new, relatively high intensity band is observed at 891 nm which can be attributed to the porphyrin dianion $[PCPP]^{2-}$, Figure 7. On the basis of the above electrochemical and spectral data, the first and second reduction of PCPP may be described by eq 1 and 2 where the Roman numerals I and II correspond to the reversible reductions shown in Figure 6a. In the presence of OH^- ions ($EtCl_2$, 0.1 M

$$PCPP + e \underset{I_a}{\overset{I_c}{\rightleftharpoons}} [PCPP^{\bullet}]^{-} \quad (1)$$

$$[PCPP^{\bullet}]^{-} + e \underset{II_a}{\overset{II_c}{\rightleftharpoons}} [PCPP]^{2-} \quad (2)$$

TBAP, 1 μM TEAH) the first reduction process is observed at $E_{1/2} = -1.10$ V which is 110 mV more positive (easier reduction) in comparison to the first reduction in neutral medium and involves one reversible electron transfer, Figure 6b. The second reduction process also occurs more easily in the presence of OH^- ions, and this is indicated by a positive (30 mV) shift of the potential. However the second one-electron-transfer process is electrochemically irreversible on the cyclic voltammetry time scale; i.e., no reoxidation peak is observed after the potential is reversed at −1.60 V. Analysis of the second reduction peak suggests that the electrochemical one-electron-transfer process is followed by a chemical step, EC mechanism.

Oxidation of PCPP—Voltammetry. Figure 8a illustrates a typical differential pulse voltammogram (DPV) for PCPP in $EtCl_2$. When potentials are scanned from zero toward the positive direction, the DPV shows three peaks. The first oxidation process (peak IIIa) is shown as a clearly defined symmetric peak at E_{pa} = 1.0 V, with the peak width at one-half peak current equal to 95 mV. The definition and symmetry of the peak and the peak width at one-half peak current indicate a one-electron-transfer process controlled by mass transport to the electrode. The second oxidation peak at E_{pa} = 1.18 V (peak IVa) is also symmetrical with the peak width at one-half peak current equal to about 95 mV but with the peak height approximately four times lower than peak IIIa. The oxidation process IV also involves a one-electron-transfer process. The third oxidation peak (peak V) is shown at peak potential E_{pa} = 1.42 V. Peak Va is clearly defined with a peak width of one-half peak current equal to 100 mV. The sum of the currents from both peaks IVa and Va is approximately equal to the current and peak IIIa which indicates that processes IV and V involve an oxidation of two species which are in equilibrium.

These three redox processes are clearly observed in cyclic voltammetry, Figure 8b. The first redox couple at $E_{1/2}$ = 0.95 involves a one-electron-transfer, diffusion-controlled, oxidation–reduction process. Diffusion control was verified by the constant value of $i_p/v^{1/2}$ and the invariant values of $E_{1/2}$ with an increase in the potential scan rate. The potential difference between the anodic and cathodic peak maxima, $E_{pa} - E_{pc}$, is equal to 60 ± 5 mV at a scan rate of 100 mV/s, thus indicating the abstraction or addition of one electron in each electron-transfer step. The abstraction of a single electron at 1.10 V was confirmed by thin-layer spectrocoulometry. However, a prolonged electrolysis (30 min) at a potential of 1.05 V, indicated the transfer of 1.6 ± 0.3 faradays of charge in process III. The second oxidation peak in cyclic voltammetry is observed at E_{pc} = 1.18 V and is irreversible on the cyclic voltammetry time scale. In DPV, the sum of the currents of peaks IVa and Va is equal to the current of peak IIIa. However, the proportion between peaks IVa and Va are different in comparison to that observed in differential pulse voltammetry; i.e., the current of peak IVa is close in value to the current of peak Va in cyclic voltammetry. This indicates that the time scale of electrolysis plays a significant role in the oxidation process of PCPP. The third one-electron oxidation process at $E_{1/2}$ = 1.4 V (peak V) is reversible on the cyclic voltammetry time

(32) Nicholson, R. S.; Shain, I. *Anal. Chem.* **1964**, *36*, 706.

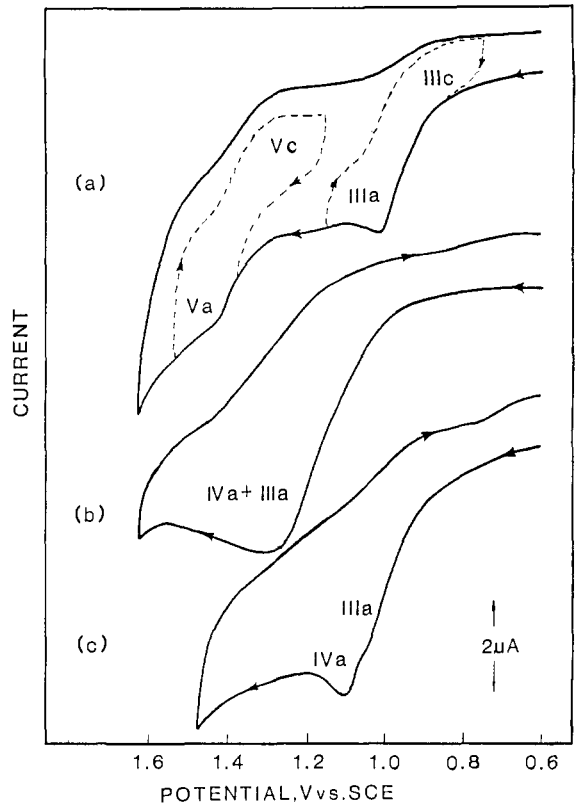

Figure 9. Cyclic voltammograms of PCPP: (a) in 1,2-dichloroethane containing 0.1 M TBAP and 1 μM acetic acid, (b) in 1,2-dichloroethane containing 0.1 M TBAP and 1 μM TEAH, and (c) in DMF containing 0.1 M TBAP. Scan rate = 100 mV/s.

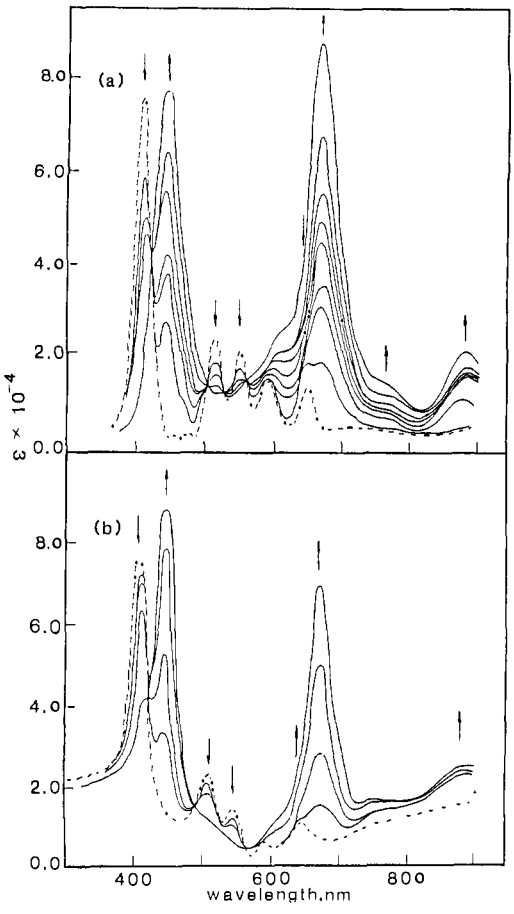

Figure 10. Thin-layer electron absorption spectra for oxidized PCPP in 1,2-dichloroethane: (a) with 0.1 M TBAP and (b) with 0.1 M TBAP and 1 μM TEAH. Dashed line shows the spectrum before electrolysis.

scale. Coulometric measurements indicate a total transfer of 2.0 faradays of charge for processes IIIa, IVa, and Va.

Oxidation of PCPP in the Presence of H^+ and OH^- Ions—Voltammetry. In order to determine the influence of protons, if any, on the electrooxidation of PCPP, voltammograms were obtained in $EtCl_2$ solution containing 0.1 M TBAP and a trace amount (about 1 μM) of acetic acid, Figure 9a. In the presence of H^+ ions, the second oxidation peak, IVa, disappears, and only two reversible couples are observed at $E_{1/2}$ = 0.97 and 1.40 V. The position of these two couples is almost identical (within 20 mV) with the position of couple III and couple V, observed in the absence of acetic acid. The cyclic voltammogram obtained in the presence of OH^- ions shows a large irreversible peak at the anodic peak potential of 1.24 V, Figure 9b. A small inflection of the current potential plot observed at 1.10 V suggests that the observed peak is due to an overlapping of two peaks. However, these peaks cannot be separated by employing a method with the capabilities of better resolution, i.e., DPV; for even with this method only one broad peak at 1.10 V (peak width at one-half peak current equal to 350 mV) is observed. The potential of this peak is between the potential of the first and second oxidation peaks, IIIa and IVa. Coulometric measurements indicate that 2.0 ± 0.1 faradays are transferred in this process. Similar irreversible, but clearly distinctive and overlapped processes are observed in DMF at anodic peak potentials of 1.02 and 1.12 V. In DMF as well as in $EtCl_2$ (0.1 M TBAP, 1 μM TEAH) solution, process Va is not observed. The environment in ethylene chloride solvent is generally considered to be more acidic in comparison to the environment in dimethylformamide solvent. This is due not only to the high electron donor capabilities of DMF in comparison to $EtCl_2$ (26 and 0.1 respectively) but also to the possible contamination of $EtCl_2$ by trace amounts of HCl from the photodecomposition of $EtCl_2$.

The presented data clearly indicate the role of acid–base equilibria in the oxidation scheme of PCPP. In basic media a chemical reaction, presumably an abstraction of protons (see following Discussion), will follow the electrochemical step.

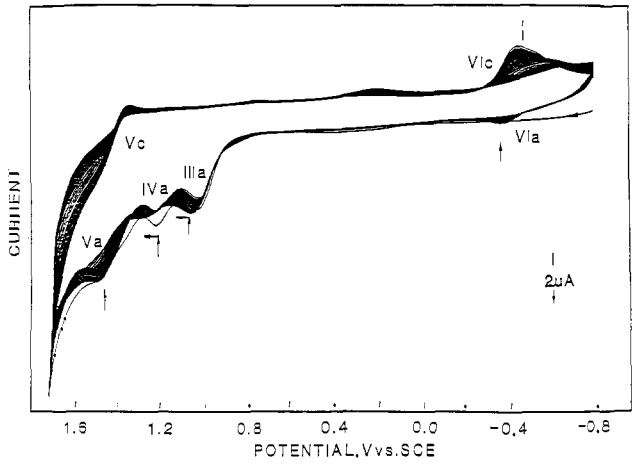

Figure 11. Continuous voltammetric scans (100 mV/s) at a Pt electrode for PCPP in 1,2-dichloroethane (0.1 M TBAP).

Spectroelectrochemistry of PCPP—Oxidation Processes. Thin-layer absorption spectra obtained during the oxidation processes of PCPP are shown in Figure 10. During the first oxidation process a new longest wavelength band appears at 883 nm. As far as the remaining bands are concerned, the 421-nm band decreases, while a new band with high absorptivity appears in the Soret region at 454 nm with a concomitant decrease of bands at 523 and 558 nm. The absorptivity of the band at 598 nm remains the same while the band at 658 nm increases and overlaps with a new band appearing at 683 nm. The absorptivity of the band at 683 nm is relatively high and is comparable with the new band which appears at 454 nm. The pattern of change with the spectrum observed during the next two oxidation steps (peak IV and V) is similar to that observed in the first step; i.e., the Soret

band at 421 nm decreases, while the high absorptivity bands at 454 and 683 nm increase and the bands at 523 and 558 nm decrease. The spectrum obtained after the third oxidation step shows only a Soret band with very low intensity and no bands at 523 and 558 nm. In addition, during the third oxidation step a bathochromic shift of the new 454-nm band to 456 nm is observed. The molar absorptivity of this band is about 5% higher than the original Soret peak but lower than the molar absorptivity of the band at 683 nm. It is surprising that the molar absorptivity of the band at 683 nm is about 20% higher than the original Soret band. The UV–visible spectrum of the product of the second and third oxidation of PCPP is significantly different from that observed for the similar oxidation of tetraphenylporphyrins.[33,34] The spectra of the latter do not contain the high absorption bands in the 600–900-nm region. It is characteristic that the bands at 683 and 883 nm (mainly of CT character) appear only in a few meso-substituted phenylporphyrins in which the functional group located on the phenyl ring can facilitate the formation of a quinoid system.[5b,c] Oxidation of TPP, which leads to the generation of the cation radical and the dication, shows in the UV–visible spectrum a decrease of the Soret band and the appearance of small bands in the range between 700 and 900 nm. A spectrum of the dication of tetraphenylporphyrins is usually poorly defined without any significant features. Therefore, the spectrum of PCPP obtained after the second or third oxidation process cannot be assigned to the dication. Even the spectrum after the first oxidation is not a clear spectrum of the cation radical. An attempt to obtain an ESR spectrum of PCPP during the first oxidation process (wave III) was unsuccessful due to the instability of the radical generated under this process. It is interesting to note that exhaustive electrolysis (1 h) at a constant potential (1.15 V) at the plateau of peak IVa, generated species with identical spectra to that which was obtained during the third oxidation process (peak V) in thin-layer spectroelectrochemistry. This is another confirmation of the existence of an acid–base type equilibrium which influences processes IV and V on the cyclic voltammetry time scale.

Oxidative Spectroelectrochemistry of PCPP in the Presence of OH^- Ions. Electrolysis of PCPP in the presence of OH^- in the potential range between 0.6 and 1.5 V (irreversible peaks III and IV in Figure 9b) shows similar spectra to that observed in neutral medium for processes III, IV, and V, i.e., a decrease of the Soret band and appearance of two high absorptivity bands at 454 and 683 nm, Figure 10b. However, contrary to the spectrum obtained in neutral medium, the proportion between the bands at 683 and 454 nm is reversed; i.e., the band at 683 nm is about 20% lower than the band at 454 nm.

Electropolymerization and Film Formation. Figure 11 shows the growth patterns for PCPP in continuous scan cyclic voltammetry from −0.8 to 1.8 V. The cyclic voltammogram clearly indicates film formation on the surface of the platinum electrode by the movement and change of current with each successive scan. While peaks IIIa, IVa, and the redox couple Va,c have been fully discussed, the new redox couple VIc,a, observed at −0.41 V, can be attributed to the reduction and oxidation of the quinone system in the PCP substituent. As the polymerization scheme proceeds, both peaks, VIc and VIa, decrease with each successive scan as the quinoid system disappears due to polymerization. No polymer film is formed on successive cycling if the potential sweep is not extended beyond 1.5 V. However, if the sweep is extended beyond 1.5 V, a polymerization and film formation of PCPP is observed. This demonstrates that the formation of the porphyrin cation radical or dication (formally) and formation of the quinoid system of bonds in PCPP (practically) is insufficient to induce polymerization of the paracyclophane groups. However, the scanning of the potential to the solvent limit, i.e., 1.60–1.65 V, causes a generation of radicals due to the oxidation of $EtCl_2$, and these radicals can in turn initiate polymerization of the oxidized form

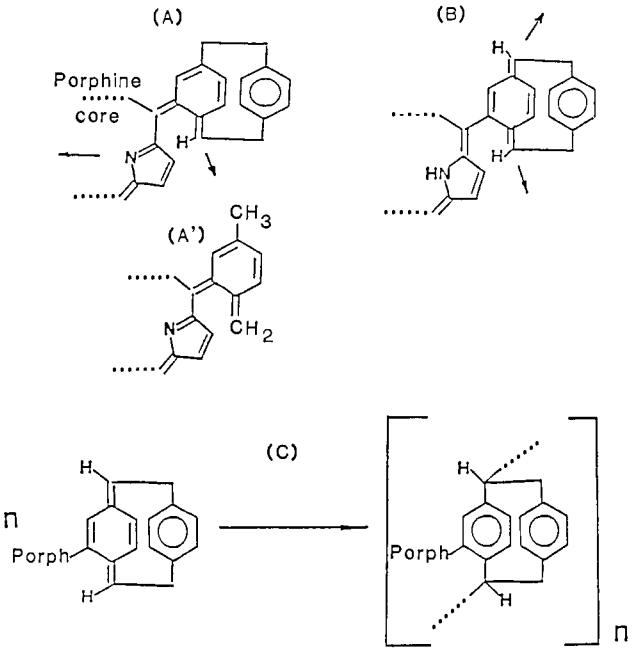

Figure 12. The models of PCPP containing the quinoid structural fragments of bonds ($PCPP_Q$) expected after removal of two H^+ from the positions denoted by the arrows. Model A′ represents the simplified model A containing the *o*-quinoid ring instead of the double-deck quinocyclophane unit.

of PCPP. The polymeric film formed on the platinum electrode is conductive with a structure similar to that observed for T(PCP)P.[5a,b] A detailed characterization of the film formed from T(PCP)P is the subject of a separate paper.[35]

Theoretical Approach to the Electrochemical Behavior of PCPP. The sequential loss of two electrons by PCPP in electrochemical oxidation is easily understandable only if the assumption is made that electrons are withdrawn from the porphyrin core with generation of the cation radical and dication.[36] This kind of mechanism is commonly accepted for the oxidation of porphyrins.[37] For what happens next, the following working hypothesis is formulated. The detachment of two H atoms from two specific atomic centers, equivalent to the loss of two protons and two electrons (as in the oxidation of hydroquinone to *p*-benzoquinone), is able to produce a quinoid system of bonds, $PCPP^{2+} \rightarrow PCPP_Q$, with the reaction proceeding via the semiquinoid intermediate. These two electrons compensate for the electron deficiency on $PCPP^{2+}$. The newly formed quinoid paracyclophanylporphyrin, $PCPP_Q$, can either (A) engage one specific NH-pyrrole ring of the porphyrin in the formation of the quinoid system with the bond joining the benzene ring directly to the porphyrin core becoming the double bond or (B) can possess the *p*-methylenequinoid system in one moiety of PCP, presumably that which is directly linked to the porphyrin core, see Figure 12. The charge transfer within the PCP unit, between the benzene ring not bonded directly with P and the ring with the quinoid system of bonds, stabilizes the latter system. The form (A) seems to be preferred over (B) because of the unusual geometry appearing in the latter[38] (strain effects, interdeck repulsion, etc.). However, form (B) can avoid excess strain by entering a polymerization scheme, see Figure 12C. In fact, the formation of polymeric film from PCPP on the electrode has been observed and would correspond to what is well known[38,39] as the transformation of *p*-xylylene to [2.2]para-

(33) Felton, R. H. *The Porphyrins*; Dolphin, D., Ed.; Academic Press: New York, 1978; Vol. 5, p 53.
(34) Malinski, T.; Chang, D.; Latour, J. M.; Marchon, J. C.; Gross, M.; Giraudeau, A.; Kadish, K. M. *Inorg. Chem.* **1984**, *23*, 3947.
(35) Bennett, J. E.; Czuchajowski, L.; Goszczynski, S.; Malinski, T., submitted for publication.
(36) Fuhrhop, J. H. *Struct. Bonding (Berlin)* **1974**, *18*, 1.
(37) Fuhrhop, J. H.; Kadish, K. M.; Davis, D. G. *J. Am. Chem. Soc.* **1973**, *95*, 5140.
(38) Liebman, J. F. "The Conceptual Chemistry of Cyclophanes" In *Cyclophanes*; Rosenfeld, S. M., Ed.; Academic Press: New York, 1983; p 43.
(39) Cordham, W. F. *J. Sci., Part A-1* **1966**, *4*, 3027.

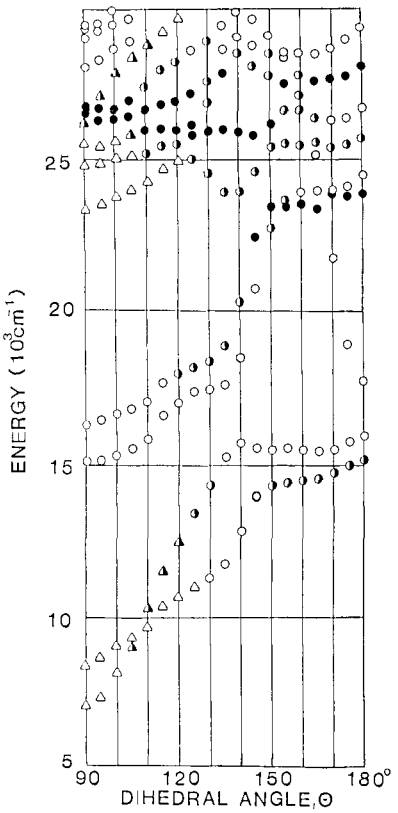

Figure 13. Excitation energy of the lowest excited states of the model A′ (see Figure 12) vs rotation angle of the attached *o*-quinoid unit. Each excited state is denoted by either triangles or circles. Triangles refer to the CT states, while circles to other states. Open triangles and circles denote the states of low intensity, $f < 0.05$; half-filled and filled symbols show respectively, the states of medium intensity, $0.05 < f < 0.5$, and high intensity $f > 0.5$.

cyclophane and accompanying polymers.

Cyclophane systems are not easily oxidized,[38] even though the formation of cation radicals and their dimers from 4,5,7,8-tetramethyl[2.2]paracyclophane[40] and [2.2](9,10)-anthracenophane[41] are known to oxidize electrolytically at low temperature. We found that [2.2]paracyclophane could be oxidized irreversibly in $EtCl_2$ at a potential of about 1.60 V. In the cation radical and dication of PCPP, the center(s) of electron-deficiency are presumed to be in the porphyrin core fragment. The possibility of the detachment of the third electron from the PCP unit would result in PCP changing to PCP$^{\bullet+}$. In such a case, however, the increase of basicity of the solution near the electrode would not enhance proton detachment. The assumption of the formation of the quinoid system of bonds in electro-oxidized PCPP can be sustained in view of the results of Bruchin et al.[40] who demonstrated by MS the tendency of the cation radical of tetramethyl[2.2]paracyclophane to form the species of *p*-xylylene and tetramethyl-*p*-xylylene (Scheme II,[40] compare our Figure 12, model B).

The calculations intended for model (A) were simplified by removing the benzene ring from PCP (A → A′). The fact that model A′ now contains the single ring, made possible the comparison of the rotation in A′ with the rotation taking place in TPP. The C–C bond lengths were taken in A′ as 1.490 A, the C=C bond lengths as 1.336 A. The CNDO/S-CIS calculations were performed for the stepwise increase of the rotation angle $\theta = 90°$ by 5° until the coplanar configuration, $\theta = 180°$, was reached. The calculated dependence of the excitation energy of the low excited states on θ values is shown in Figure 13. It can be seen

(40) (a) Bruhin, J.; Gerson, F.; Ohya-Nishiguchi, H. *Helv. Chim. Acta* **1977**, *60*, 2471. (b) Bruhin, J.; Gerson, F.; Ohya-Nishiguchi, H. *J. Chem. Soc., Perkin Trans. 2* **1980**, 1045.

(41) Gerson, F.; Kaupp, G.; Ohya-Nishiguchi, H. *Angew. Chem., Int. Ed. Engl.* **1977**, *16*, 657.

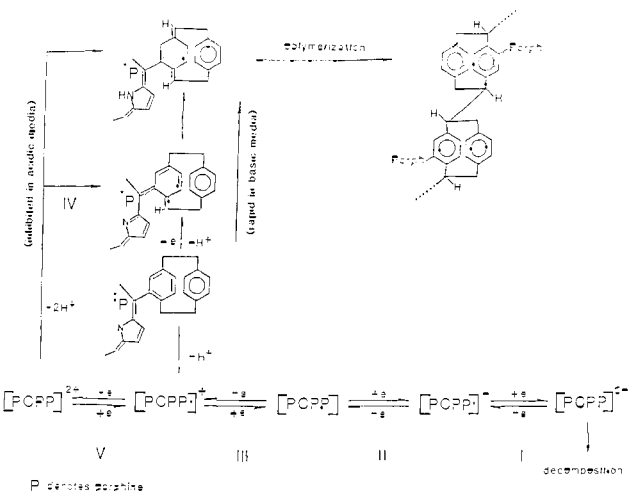

Figure 14. Reaction pathway for the electrochemical oxidation and reduction of PCPP.

that (i) the excitation energy of the four lowest excited states is extremely sensitive to the changes of θ, (ii) the gradual increase of the excitation energy takes place for these states in the range of θ, 90°–150°, while the magnitude of the increments decreases in the range of θ, 150°–180°, (iii) the remaining excited states are less sensitive to the θ changes and are characterized by an alternate increase and decrease of excitation energies. These results are different from those formulated on the basis of Figure 5 for TPP. However, some common features appear. First of all, for both the perpendicular and coplanar configuration of A′ and P units, two excited states appear in the 15 000–16 000-cm^{-1} region, as in the case of TPP. Although their splitting is more limited, the low intensity values suggest a similar origin, and the states are, therefore, the Q states of P. A similar occurrence is observed with the higher energy states in the 24 000–28 000-cm^{-1} region. The large energy gap which separates the higher energy states from the Q states as well as the high intensity allows us to consider them as the B states of P. It is characteristic that the states which represent B states for $\theta = 90°$ become the Q states for $\theta = 180°$. The similarity between the two lowest energy states deserve a more detailed description.

It can be seen in Figure 13 that for the θ interval of 90°–150° the two energetically lowest excited states greatly increase in energy as well as in intensity from the range 7000–8000 to 14 500–15 500 cm^{-1}. For the state of the lowest excitation energy, the oscillator strength increases slightly from $f = 0.005$ to $f = 0.069$. The adjacent state of higher energy represents a greater oscillator strength, $f = 0.014$ for $\theta = 90°$. With an increase of the rotation angle at $\theta = 125°$, $f = 0.444$ and the oscillator strength begins to decrease gradually. As the analysis of the transition density matrix demonstrates, both states have CT character but only for the θ interval 90°–125°; the charge transferred from the porphyrin fragment to the quinoid substituent equals $\Delta q = 0.92$–0.49 e for the first state and $\Delta q = 0.94$–0.56 e for the second state. For $\theta > 130°$ these states are no longer exclusively CT states. This means that both states of lowest energy, which at the beginning of the rotation were CT states, now become the Q states of the porphyrin.

There is no reason not to assume for the model containing the A′ unit the same geometry which characterizes the paracyclophanylporphyrin, PCPP, with the θ value in-between the perpendicular and coplanar configurations. For such a configuration, the presented discussion can be applied to the explanation of the changes occurring in the UV–vis spectra during the electrochemical processes monitored by thin-layer spectroelectrochemistry. The modified spectra show (i) the presence of a new absorption band of low intensity at 883 nm, (ii) a bathochromic shift of the long wavelength component of the Q band (α-band) from 658 to 683 nm connected with a substantial increase of intensity, (iii) the appearance of a new, highly intense band of absorption at 454 nm in the vicinity of the B band (Soret), the latter re-

maining at 421 nm but with very low intensity. These experimental data are in agreement with the results of the calculations performed for $\theta = 130°$. The longest wavelength transition at 886 nm, $f = 0.017$, can be related to the longest wavelength band of low intensity. To the second longest wavelength transition, at 697 nm, $f = 0.342$, one can ascribe the component of the Q band, gaining intensity, see (ii). Specific properties of both transitions result from the importance of the charge transfer from the porphyrin to quinoid unit. The new band near the B band represents the band which appears in the calculations performed for PCPP as the doubly excited A → B transition. In the considered case it shows a much greater split. This split cannot take place for the discussed model because it originates from the nature of the substituent present in the system. Therefore the A → B transition at 385 nm, $f = 1.669$, can be assigned only to the Soret band.

An overall oxidation–reduction scheme for the investigated PCPP is shown in Figure 14. This self-consistent scheme is postulated on the basis of the observed electrochemical and spectrochemical data which is supported by theoretical calculations. The reduction processes of PCPP are typical for other meso-substituted porphyrins. However, the interesting and significant aspect of the oxidation mechanism of PCPP is that oxidation appears to occur initially at the porphyrin core and due to internal electron transfer is shifted to the paracyclophane substituent. The oxidation of the paracyclophane substituent involves the detachment of protons, and this process can be significantly accelerated in basic and inhibited in acidic media.

Conclusions

The formation of the paracyclophane–porphyrin link resulted in far-reaching changes of the electronic structure of both components. The increased energy of the HOMO and HOMO–1 of the porphyrin core, P, as compared to TPP took place together with the filling of the energy gap in P levels by the highest occupied MOs of PCP. The appearance of singly excited configurations from the HOMO and HOMO–1 of PCP to the LUMO and LUMO+1 of P in the split excited B states of PCPP was observed. The calculations reproduced the trends in the experimental data pointing to the bathochromic shifts in all Q and B bands; these shifts increased in the order P < TPP < PCPP. For the excited states the increase of the CT% numbers was apparent. According to calculations based on the transition density matrix formalism, this increase took place in the same order due to the LE% (local excitation) numbers. The role of the paracyclophane–porphyrin interaction increased in the B excited states as demonstrated by the CT% numbers. This interaction represented one-half of the CT% numbers in the excited B state for which the charge transfer from PCP to P amounted to 0.38 e. In the cyclic voltammograms of PCPP three oxidation processes appeared which corresponded to a gradual transport of electrons of which the first oxidation potential was characterized by the low value of $E_{1/2} = 0.95$ V. These changes were accompanied by a significant bathochromic shift, increased intensity of the longest wavelength absorption band, and the appearance of a split Soret band. It is assumed that after the first two steps, PCPP → $PCPP^{\bullet+}$ → $PCPP^{2+}$, the flow of two electrons from PCP to P combined with the detachment of two protons resulted in the formation of the quinoid system of bonds, possibly across the paracyclophane–porphyrin link.

The novel system of *meso*-[2.2]paracyclophanyltriphenylporphyrin, PCPP, behaves, therefore, as an electron-flexible system where in the B excited states (Soret band), the PCP substituent acts as the electron donor and the porphyrin core (with three phenyls attached) as an electron acceptor. However, under the dynamic conditions of electron transfer from PCPP to the electrode, monitored by spectroelectrochemistry and cyclic voltammetry, after $PCPP^{2+}$ + 2e step and the formation of the quinoid $PCPP_Q$, the situation in the latter becomes reversed: the moiety of PCP directly joined to the porphyrin core behaves as the electron acceptor fragment, while the porphyrin core and the second ring of PCP behaves as the electron donors. The fact that the planes of the porphyrin core and the quinoid ring, directly joined to the latter, form an angle in-between the coplanar and perpendicular conformations, resulted in the spectral changes observed in PCPP. These changes consisted of the split of the Soret band (reaching a maximum for the coplanar conformer) and a bathochromic shift of the longest wavelength absorption band Q (at a maximum for the perpendicular conformation).

This suggested model for the intramolecular electron transfer from the paracyclophane unit to the porphyrin unit in PCPP could apply to other porphyrin derivatives particularly to *meso*-tetrakis[2.2]paracyclophanylporphyrin, T(PCP)P.[4ab,5] However, it could also apply to meso-substituted porphyrins in which functional groups located on the phenyl substituent, due to the resonance effect of lone pair electrons could facilitate the formation of a quinoid system (e.g., *meso*-tetrakis(3-methoxy-4-hydroxyphenyl)porphyrins).[5a] The formation of the quinoid structural fragment in both PCPP and T(PCP)P seems to be responsible for formation of the polymeric films on the electrode. These films were conductive[5] and show catalystic properties with regard to the reduction of oxygen in both acidic and basic media. These facts, together with the unusual lowering of the oxidation potential (the attachment of four paracyclophane substituents to the porphyrin ring shifts the first oxidation potential approximately 510 mV more negative in comparison to the first oxidation potential of TPP) and broadening of the spectrum in the visible region could give the chance to use the immobilized polymeric (metallo)-porphyrins derived from PCPP in energy conversion and storage devices and also in electrocatalysis.[42]

Registry No. PCPP, 117439-49-3.

(42) Czuchajowski, L.; Malinski, T., manuscript in preparation.